Transforming complex multistability to controlled monostability

Binoy Krishna Goswami*
Laser and Plasma Technology Division, Bhabha Atomic Research Centre, Mumbai 400085, India

Sourish Basu†
Department of Physics, Indian Institute of Technology, Mumbai 400076, India

(Received 25 August 2001; revised manuscript received 21 May 2002; published 27 August 2002)

Multistability, a commonly observed feature among nonlinear systems, could be inconvenient under various circumstances. We demonstrate that a control in the form of slow and weak periodic parameter modulation can be effectively applied to transform a complex multistable system to a controlled monostable one. For the representative of a nonlinear system, we choose the Hénon map as the standard model. The number of coexisting stable states is known to increase as the dissipativity reduces. We show that even in the low dissipative limit, when the number of coexisting states could be arbitrarily large, the periodic parameter modulation can destroy the states coexisting with stable period 1. Thus, the system can be brought from any other branch to period-1 branch, leading to controlled monostability. This method works in the presence of noise as well.

DOI: 10.1103/PhysRevE.66.026214 PACS number(s): 05.45.Ac, 05.45.Gg, 05.45.Pq

Nonlinear dynamical systems, having large dimension (in the phase space) or (and) under low dissipation, commonly exhibit multistability, i.e., coexistence in the phase space of several stable states (sinks) when the system parameter values remain unchanged. Systems with two sinks (bistability) and the associated hysteresis are well known. A more complex form of multistability (several periodic or chaotic states) has also been observed in various systems, including CO_2 lasers [1–4], semiconductor lasers [5–7], nonlinear electronic circuits [8], voltage controlled buck converter [9], the Rayleigh-Bernard experiment [10], thermal hydraulics in two-phase natural circulation loops [11], cardiac dynamics [12], and periodically stimulated neuron [13]; in addition to some standard models, under periodic forcing or parametric excitation, such as Duffing, van der Pol [14], and Toda oscillators [15,16].[1] Under several circumstances, multistability can create inconveniences. We outline very briefly some of these issues.

(i) If a system is designed to remain at a certain dynamical equilibrium, a jump to a coexisting sink may change the performance and spoil the reproducibility and hence reliability. We believe there are many applications (devices) where multistability should therefore be avoided. For instance, rapid progress has been taking place in research and technology development in the area of optical fiber communication [17,18]. This has led to the development of a variety of semiconductor lasers (amplifiers), doped fiber lasers (amplifiers), in addition to vast improvement in optical fiber technology and other accessories. A very basic phenomenon involved in optical fiber communication is signal transmission (amplification) through a light-wave carrier. This process may be compared to the dynamics of a driven nonlinear system which can exhibit multistability. Indeed, semiconductor lasers, and (doped) optical fibers exhibit a wealth of nonlinear optical phenomena [18], including various bifurcations, chaos [19], and multistability under current (pump) modulation [5] or optical injection [6,7]. We believe, multistability would pose inconvenience in efficient communication and thus needs to be avoided.

(ii) In some applications, in addition to reliability and reproducibility, the more important issue is the safety of the installation and the neighborhood. As an example, we refer to the two-phase natural circulation loops that have many applications including the future generation natural circulation nuclear reactors [11,20]. In nuclear reactors, the coolant flow design is crucial to avoid all sorts of instabilities that may lead to a holocaust. Therefore, multistability might be inconvenient while designing the operating regime (the permitted region of operation in the parameter space) of the coolant flow.

(iii) A deterministic nonlinear dynamics approach has entered various disciplines, including Cardio Science. The transition from a normal cardiac rhythm to arrythmia has been observed to follow period doubling route to chaos [21]. Cardiac alternans (period-2 rhythm) could be a precursor to arrythmia and therefore efforts have been made to devise some controls. Indeed, the chaos control [22] and tracking [23] techniques have been successfully applied to suppress cardiac alternans and stabilize the cardiac rhythm in the unstable period-1 state [24]. Notably, under certain circumstances, a stable period-2 rhythm can coexist with the stable period 1 [12]. In such cases, changing the cardiac rhythm back to stable period-1 state might be an attractive proposition.

Thus we have briefly mentioned some of the areas where multistability would be undesirable. Such disturbances often

*Email address: bgoswami@apsara.barc.ernet.in
†Email address: n9026014@ccs.iitb.ac.in

[1]The primary origin of multistability in periodically forced nonlinear systems may be sought in harmonic and various subharmonic resonances. The overlap of these resonances in the parameter space gives rise to multistability.

also restrict the operating regimes of the system. Also, problems can become more acute when the basin boundaries become fractal [25]. Because, under such circumstances, if the transients place the system close to a basin boundary, even noise (which is unavoidable in many experimental and real-life systems) can lead to a transition from one basin to another. In order to control multistability, Poon and Grebogi [26] have proposed a method where the system is placed into (or removed from) some sink by applying noise and feedback control. In spite of its applicability in general, under certain circumstances, some difficulties may still remain. For instance, if we want to bring the system to the stable period 1 from a coexisting sink by some fast and deterministic method, then the application of noise may not be an efficient proposition. An alternative approach could be transforming the multistable system to a monostable one by some control mechanism. Pisarchik and Goswami [27] have recently proposed a method of converting a bistable system to a controlled monostable system by a slow and weak modulation of some system parameter. They have theoretically demonstrated the method in the Hénon map [28] and laser rate equations [29], and experimentally realized in a CO_2 laser. In the experiments, the CO_2 laser was made bistable by a cavity loss modulation. Next, the bistability is controlled by a slow and weak modulation of resonator cavity length. The basic idea in this controlling method is to introduce a collision of the undesirable state with its basin boundary (the stable manifold of the neighboring saddle), so that such a state is destroyed and the transients settle down to the desired basin.

In the current paper we study the applicability of this technique when the system exhibits coexistence of an arbitrarily large number of coexisting sinks. For the representative of a nonlinear system, we choose the Hénon map [28] described by $x_{n+1}=1-\mu x_n^2+y_n$, and $y_{n+1}=-Jx_n$.[2] The Hénon map is considered as a standard theoretical model for the continuous-time experimentally realizable (real-world) systems. The iterates x and y may be considered as two projected dynamical variables. The parameter J may be related to the dissipativity, and μ represents an externally controllable parameter. The Hénon map and Toda oscillator[3] have shown striking similarity in the self-similar organization of the secondary cascades [16,35]. Such similarity could be because both have a similar hyperbolic horseshoe [36]. Notably, the bifurcation structures of a large number of driven nonlinear systems, including the Duffing and Toda oscillators, exhibit qualitative similarity [37]. Therefore, the Hénon map might be all the more suitable for the driven low-dimensional systems, e.g., CO_2 and semiconductor lasers, nonlinear electronic circuits, etc. We also expect that the technique demonstrated in the Hénon map may as well be effective in controlling multistability in other nonlinear systems including cardiac rhythms, and thermal hydraulics.

The number of coexisting attractors is known to increase as the dissipativity of the system reduces. We consider the extreme situation, i.e., at the near-conservative (low-dissipative) limit when the number of coexisting states could be arbitrarily large. We show that even under such circumstances, the periodic modulation of some system parameter may be effectively applied to transform such an exceedingly complex multistable system to a controlled monostable one. We also demonstrate the applicability of the method in the presence of noise.

Since the Hénon map is a two-parameter map, the order of occurrence of the sinks (as one changes the value of μ for a given value of J) can change as the value of J changes [38]. However, the sinks are not created in a totally arbitrary manner. Mindlin *et al.* [39] have shown (by means of a horseshoe implication diagram) that a minimal set of periodic orbits can be constructed, which force the existence of all the remaining periodic states associated with a strange attractor, up to any given period. In fact, a large class of periodic and chaotic orbits are created in the phase and parameter space in an organized manner [35]. We explain the organization in brief to highlight the associated complex multistability. We consider a low dissipative case ($J=0.98$) and increase the value of μ as the control parameter. Figure 1(a) shows the bifurcation diagram of the period-1 branch (denoted by p_1). Notably, around each sink of the period-1 branch, an infinitely large series of period n-tupled saddle nodes seems to appear in the following sequence ($n=\ldots,5,4,3$). Each newly born node (say of period n) later constitutes its own branch (first-order secondary cascade), denoted by p_n. For instance, period-5, -4, -3 cascades are shown to coexist with period 1 in Fig. 1(b). Again, around each sink of every secondary cascade, an infinitely large series of period n-tupled saddle nodes seems to appear following the same sequence. Each node later constitutes its own branch (second-order secondary cascade). For example, Fig. 2(a) shows period-20, -16, -12 cascades, each coexisting with the period 4 of period-4 branch. Figure 2(b) shows period-25, -20, -15 cascades, each coexisting with the period 5 of period-5 branch. These processes recur in a self-similar manner, giving birth to higher and higher-order secondary cascades; more evidence of the creation of higher-order cascades may be seen in Ref. [35]. Each cascade survives within a small subinterval of the control parameter window where the respective sink from the immediate lower-order secondary cascade exists. Thus, subject to the choice of parameter values, the number of coexisting sinks could be arbitrarily large. In principle, in an infinitely large number of parameter values, there could be an infinitely large series of coexisting sinks. This scenario suggests an exceedingly complex multistability, although organized in a self-similar manner.[4]

[2]The Hénon map reduces to one-dimensional quadratic map for $J=0$. Multistability occurs when $J>0$ [30].

[3]The Toda oscillator is a well-known model of CO_2 and semiconductor lasers. The recent experiments on multistability in periodically forced CO_2 laser [4] have shown good agreement with the theoretical predictions [15] on the basis of the Toda oscillator model [31] of laser rate equations [1,32]. Moreover, laser rate equations of semiconductor lasers [5], and vibro rotational model of CO_2 lasers [33,34] also reveal the Toda oscillator form.

[4]The creation of sinks is in good agreement with the predictions of Gavrilov and Silnikov [40], Newhouse [41], and Robinson [42]. More detail in this regard may be seen in Ref. [35].

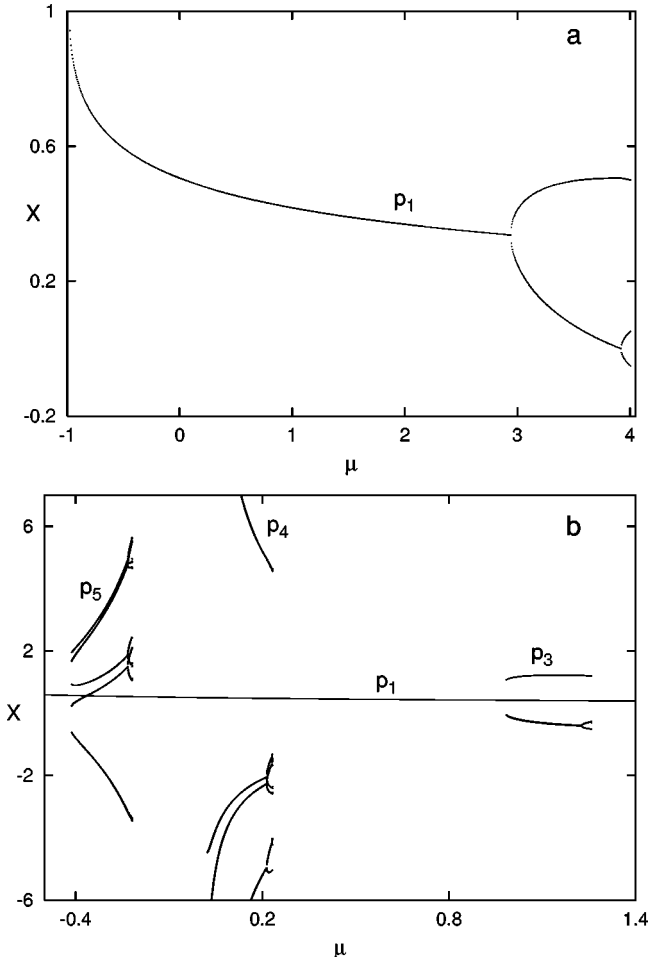

FIG. 1. (a) Bifurcation diagram of the period-1 branch (p_1). (b) Successive appearance of a series of first-order secondary cascades, namely, period -5, -4, and -3 branches, around the period 1.

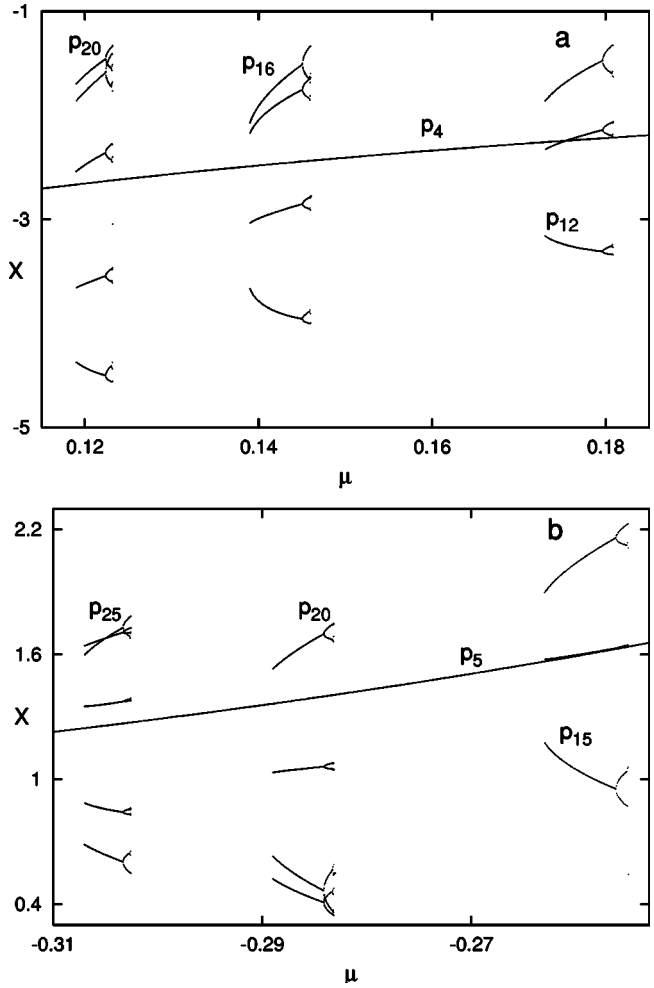

FIG. 2. Successive appearance of second-order secondary cascades around the period-4 sink of p_4 branch, and around the period-5 sink of p_5 branch. (a) Period-20, -16, -12 cascades around period 4. The sampling period is four. (b) Period-25, -20, -15 cascades around period 5. The sampling period is five.

We apply sinusoidal control modulation over μ as $\mu(n) = \mu_0 + \eta \sin(2\pi\nu n)$. By ''slow'' modulation we imply that the period of modulation $(1/\nu)$ is much larger than the period of the sink to be controlled. Also, by ''weak'' modulation we imply that the addition of η over μ in the uncontrolled case will lead to no bifurcation of the sink. We demonstrate that if the system exists in any secondary cascade, one can destroy that cascade by control (in the form of a slow and weak periodic modulation over μ) and bring the system to the period-1 branch. Since within a branch, the largest parameter window is that of the first sink, for control we choose the value of μ_0 such that the uncontrolled case refers to the first sink of the given secondary cascade to be destroyed.[5] We shall see later that the control modulation induces the destruction of the sink after the creation of a sequence of period doubling in control frequency. After destruction, the chaotic transients jump to the basin of the neighboring sink from the immediate lower-order secondary cascade. In the following figures where we show the controlled scenario, the controlled first sink of a p_n branch is also denoted by p_n. Each bifurcation diagram of the controlled p_n has been plotted with sampling period $(1/\nu)$. We demonstrate some examples of controlled destruction starting from second-order secondary cascades. Figure 3(a) shows the controlled destruction of p_{12} and subsequent jump to p_4. Figures 3(b) and 3(c) show a similar controlled destruction of p_{16} and p_{20}, respectively. Each destruction is followed by a transition to p_4. In Fig. 3(d), the values of μ_0 and ν have been kept same as in the case of p_{16} destruction. Next by increasing η, p_4 gets destroyed and the chaotic transients jump to period 1 (p_1). A similar destruction of p_4 also occurs when the value of μ_0 is set anywhere, including in the parameter subintervals where other second-order secondary cascades, viz., p_{12} and p_{20} exist. Figures 4(a–c) show similar destruction of p_n $(n = 15,20,25)$ branches respectively. In each case, the system jumps to p_5. In Fig. 4(d), we keep the values of ν and μ_0

[5]Other sinks of a given branch can also be destroyed by a similar control. Under such circumstances, the value of μ_0 has to be chosen such that the uncontrolled case refers to the given sink. In general, the required control amplitude to destroy these sinks is much less than that required for the destruction of first sink.

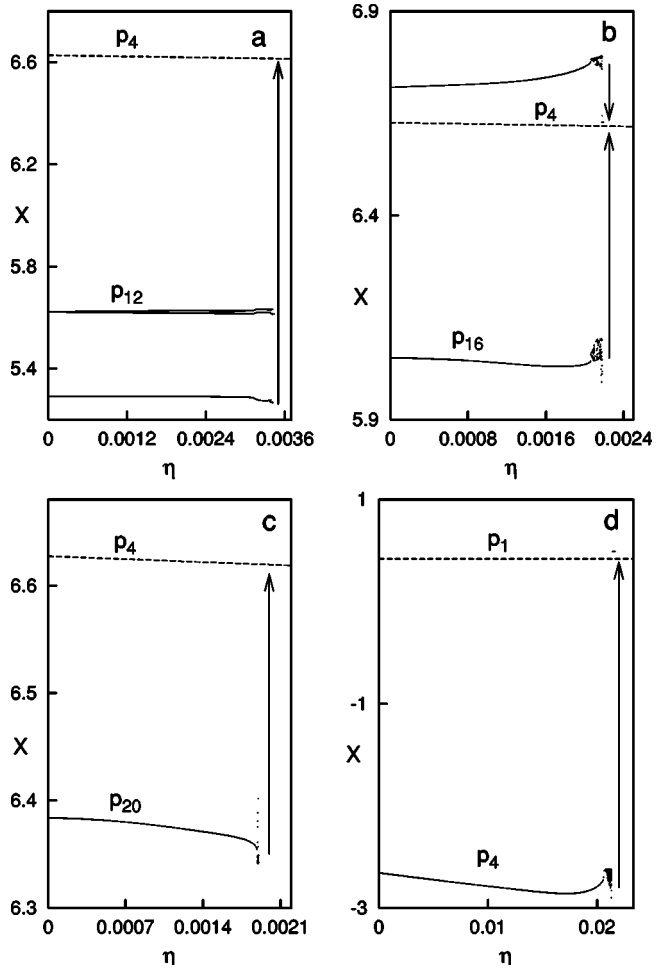

FIG. 3. (a)–(c) Bifurcation diagrams show the controlled destructions of some second-order secondary cascades, born around period 4; $\nu=0.005$. (a) p_{12} ($\mu_0=0.177$), (b) p_{16} ($\mu_0=0.142$), and (c) p_{20} ($\mu_0=0.121$). After each destruction, the transients jump [shown by arrow(s)] to period 4 (p_4). (d) Bifurcation diagram of controlled period 4 (p_4) shows its destruction and jump to period 1 (p_1); $\mu_0=0.142$; $\nu=0.005$. Enlargements of the bifurcation diagrams in plots (a) and (d) are shown later in Figs. 5(a) and 5(b), respectively.

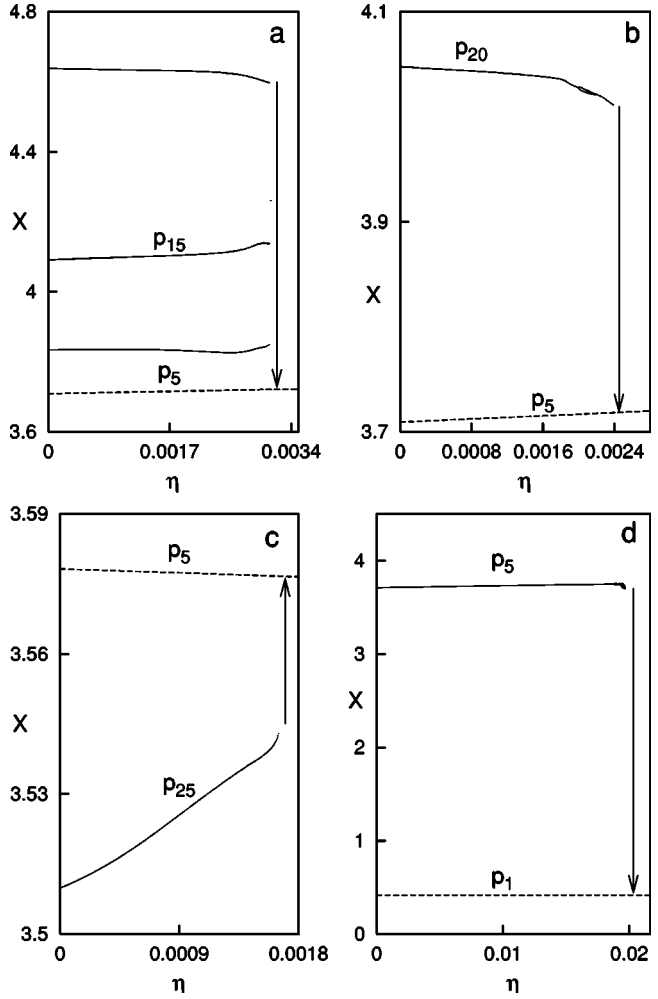

FIG. 4. (a)–(c) Bifurcation diagrams show controlled destructions of some second-order secondary cascades, born around period 5 (p_5); $\nu=0.005$. (a) p_{15} ($\mu_0=-0.259$), (b) p_{20} ($\mu_0=-0.286$), (c) p_{25} ($\mu_0=-0.305$). After each destruction, the chaotic transients jump (shown by an arrow) to period 5. Enlargements of bifurcation diagrams in plots (a) and (b) are shown later in Figs. 5(c) and 5(d). (d) Bifurcation diagram of controlled p_5 shows its destruction and transition (shown by an arrow) to period 1 (p_1); $\mu_0=-0.286$; $\nu=0.005$.

same as in the case of p_{20}. Then by increasing η, p_5 is destroyed and the transients jumps to period 1. A similar destruction of p_5 can also be observed when the value of μ_0 is set anywhere, including in the parameter subintervals where other second-order secondary cascades, viz., p_{15} and p_{25} exist. In Fig. 5, we show enlargments of the previously shown bifurcation diagrams to illustrate the sequence of period doubling in control frequency before the destruction. Figures. 5(a) and 5(b) show the magnified results of controlled p_{12} and p_4, respectively. In each case, one notices a period doubling route(s) to chaos. The lifetime of the chaotic transient depends on how far the chosen parameter value is from the respective boundary crisis threshold [30]. Therefore, if the value of the control amplitude is sufficiently over the destruction threshold, the time span of chaotic transients can be reduced significantly. Moreover, a jump to a lower-order cascade does not always need the system to become chaotic as a precursor. Such a jump can occur even prior to chaos. For instance, Fig. 5(c) shows that no period doubling occurred in controlled p_{15} before the jump to p_5. Figure 5(d) shows that the controlled period 20 undergoes just two steps of period doubling followed by two steps of an inverse period doubling before being destroyed in a similar manner.

Figure 6 shows the destruction curves of these cascades in (η versus ν) parameter subspace; we consider the case of the destruction of first sinks only. In Fig. 6(a–c) we compare the destruction thresholds of some second-order secondary cascades versus those of the respective first-order secondary cascades. The destruction curve of a second-order cascade, say p_n, is denoted by C_n. $C_{m,n}$ represents the destruction curve of the period-m branch (a first-order secondary cascade) when μ_0 is kept same as in the case of the destruction

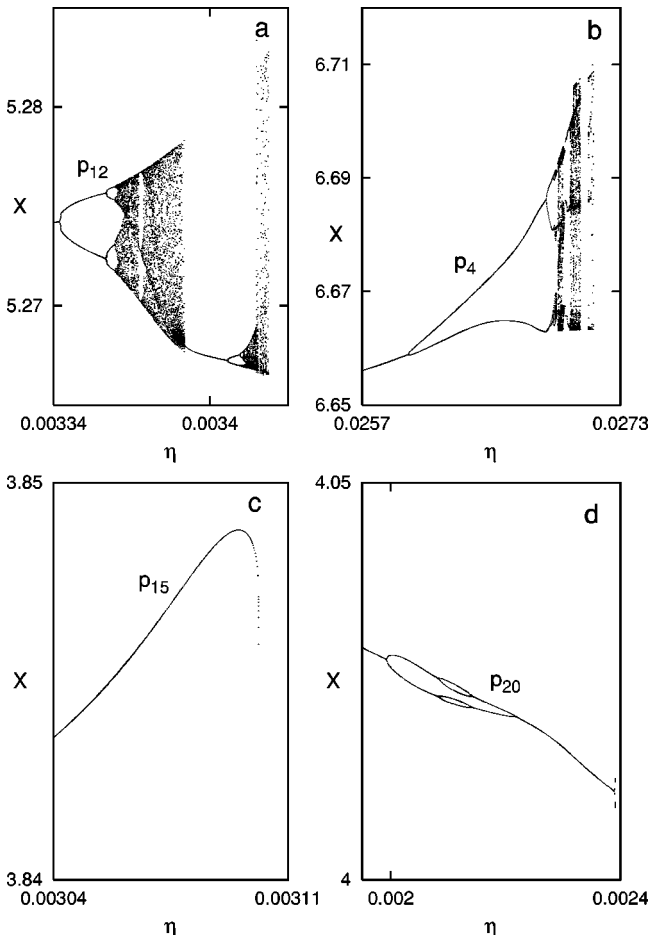

FIG. 5. Enlargements of some bifurcation diagrams shown earlier in Figs. 3 and 4; $\nu=0.005$. (a) p_{12} ($\mu_0=0.177$), (b) p_4 ($\mu_0=0.142$), (c) p_{15} ($\mu_0=-0.259$), and (d) p_{20} ($\mu_0=-0.286$). (a) and (b) show period doubling route to chaos. (c) Controlled period 15 does not undergo any period doubling. (d) Controlled period 20 undergoes just two steps of period doubling followed by two steps of inverse period doubling.

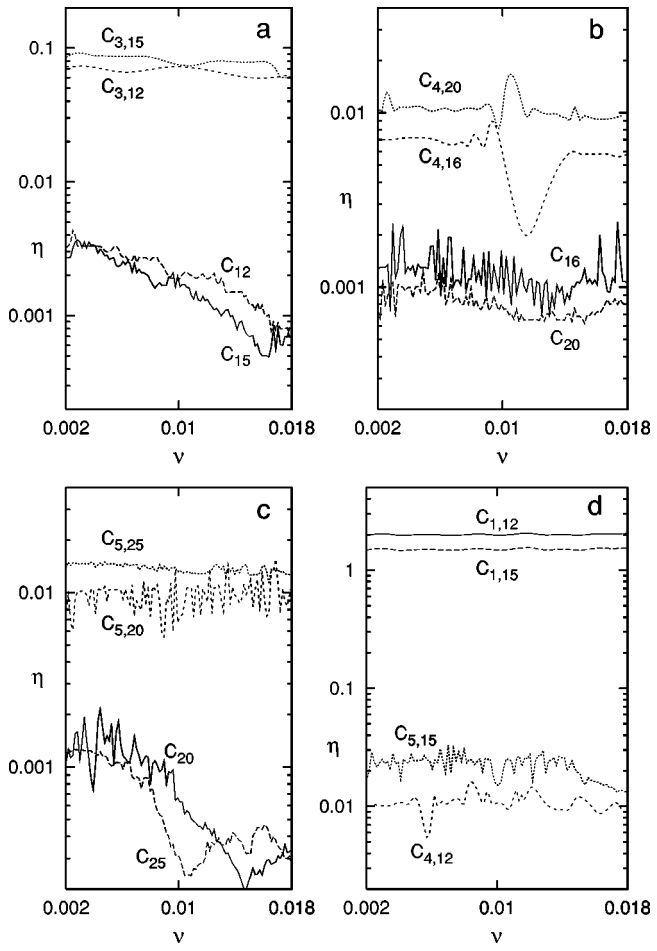

FIG. 6. Controlled destruction curves, denoted by C_n or C_{nm}. (a) Period 12 ($\mu_0=1.103$), period 15 ($\mu_0=1.072$), and period 3 at both the μ_0 values. (b) Period 16 ($\mu_0=0.142$), period 20 ($\mu_0=0.121$), and period 4 at both the μ_0 values. (c) Period 20 ($\mu_0=-0.286$), period 25 ($\mu_0=-0.305$), and period 5 at both the μ_0 values. (c) Period 4 ($\mu_0=0.177$), period 5 ($\mu_0=-0.259$), and the controlled period doubling ($1\rightarrow2$) bifurcation curves at both the μ_0 values.

of p_n branch (a second-order cascade). For instance, in Fig. 6(a), the destruction curves of period 12 and period 15 are denoted by C_{12} and C_{15}, respectively. This plot also shows the destruction curve of p_3 branch when μ_0 is kept the same as in the case of the destruction of p_{12} and p_{15} branches. These destruction curves are denoted by $C_{3,12}$ and $C_{3,15}$, respectively. This plot reveals that for a broad range of modulation frequency, p_{12} and p_{15} can be destroyed at a lower modulation amplitude in comparison to that required for p_3 destruction. Similarly plot (*b*) reveals that the destruction thresholds of p_{16} and p_{20} are much smaller in comparison to that required for p_4. Plot (c) shows that the destruction thresholds of p_{20} and p_{25} are much smaller in comparison to that required for p_5. Thus, for any modulation frequency, if one increases the control amplitude appropriately, the second-order cascades can be destroyed and the chaotic transients would settle in the respective first-order cascades. In plot (d), $C_{1,12}$ and $C_{1,15}$ denote the bifurcation curves for period doubling from period 1 when the values of μ_0 are kept same as in the case of the destruction of p_{12} and p_{15}, respectively. $C_{4,12}$ denotes the destruction curve of p_4 when the μ_0 is kept same as in the case of p_{12}. Similarly, $C_{5,15}$ denotes the destruction curve of p_5 when the μ_0 is kept same as in the case of p_{15}. Plot (d) shows that the controlled period doubling from period 1 requires a much larger value of η in comparison to those required for the destruction of p_4 and p_5.

Thus our observations suggest the following features in general.

(i) The control amplitude to destroy a given nth-order secondary cascade is much less in comparison to that required for the destruction of the neighboring $(n-1)$th-order secondary cascade. Consequently, after the destruction of the nth-order secondary cascade, the system jumps to the respective $(n-1)$th-order secondary cascade.

(ii) The control amplitude required for period doubling $(1\rightarrow2)$ in the period-1 branch is much larger in comparison to that required for the destruction of any first-order secondary cascade. As a consequence, after the destruction of a

first-order secondary cascade, the system jumps to the period-1 branch.

Therefore, if we know the period of the state to be destructed, we can set some appropriate slow control frequency and then as we increase the control amplitude beyond the respective destruction threshold, the state can be destroyed and the system will jump to the immediate lower-order secondary cascade. Again by increasing the control amplitude further, the new state can also be destroyed and the system will then jump to a further lower-order secondary cascade. Subject to enough increase of the value of η, this process can go on in a recursive manner till the system jumps to the period-1 branch. This process does not require any *a priori* information about the destruction threshold of various secondary cascades. It needs a gradual increase of the control amplitude and monitoring till the system returns to the period-1 branch. In this process, the transition to p_1 will occur via a sequence of jumps among the hierarchy of secondary cascades, viz., the nth-order secondary cascade $\rightarrow$ $(n-1)$th-order cascade $\rightarrow \ldots \rightarrow$ first-order cascade $\rightarrow p_1$. Such jumps within secondary cascades can be reduced and the system can be straightway brought to any lower-order (say nth) secondary cascade (period-1 branch) when the destruction threshold of the respective $(n+1)$th (first) -order secondary cascade is known *a priori*. Then the control amplitude can be set straightway higher than the destruction threshold of the respective $(n+1)$th (first) -order cascade. This would lead to a direct transition to the nth secondary cascade (period-1 branch) instead of a sequential transition through the secondary cascades. We shall show some examples of such a direct transition to period-1 branch in Fig. 11.

To show the applicability of the control in the presence of noise, we introduce Gaussian white noise (ξ and ϕ) in the Hénon map as follows: $x_{n+1}=1-\mu x_n^2+y_n+\xi_n$, and $y_{n+1}=-Jx_n+\phi_n$. We consider for simplicity both noise terms having zero mean and identical standard deviation (σ). Subject to the strength of noise (determined by the standard deviation), the dynamics of a nonlinear system, in general, could be complex. This is where the basins of attraction play a significant role. Noise of adequate strength can induce a spontaneous transition from one basin to another. Even the system may get further disturbed, leading to intermittent transitions among the coexisting basins. On the other hand, if a basin is broad enough, scenario could be different. Under such circumstances, even though noise can induce randomness (and hence transients), the dissipativity of the system would always attempt to pull and retain the system back within the same basin. As a consequence, no such transition or intermittancy may occur. We have studied the basins of various secondary cascades in the Hénon map.[6] The basins of higher-order secondary cascades appear and always remain within the basins of the immediate lower-order secondary cascades. Higher the order of the cascades, smaller their basins become progressively. Consequently, the effect of noise would be more prominent for the higher-order secondary cascades. We will show later a strong noise-induced transition (without control) from higher-order to lower-order secondary cascades. First we analyze the effect of moderate noise when no such transition takes place. Figure 7(a) shows the bifurcation diagram of the uncontrolled p_{16} branch (around period 4 of p_4 branch) in the presence of noise ($\sigma=0.001$). Past the boundary crisis of p_{16}, the transients converge to p_4. Since, the basin of period 4 is comparatively larger, the p_4 branch can withstand a relatively stronger noise. Figure 7(b) shows the bifurcation diagram of p_4 around period 1 when the standard deviation of noise is relatively high ($\sigma=0.005$). Beyond the boundary crisis of p_4, the transients settle to period 1 [Fig. 7(b)]. We demonstrate

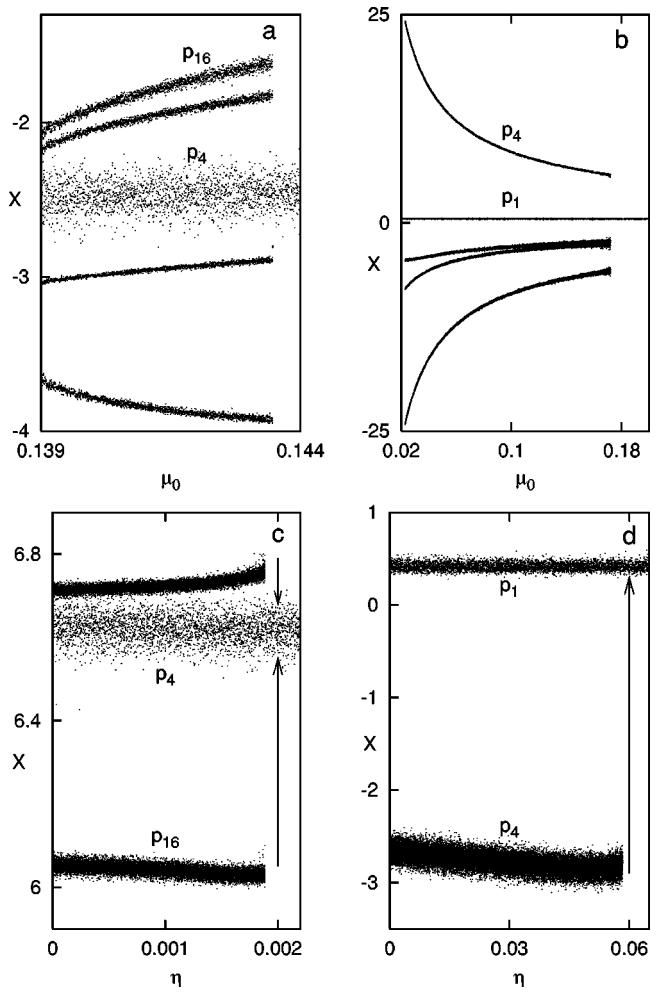

FIG. 7. (a) Uncontrolled period-16 branch (p_{16}) around period 4 (p_4) in the presence of noise ($\sigma=0.001$). Sampling period is four. (b) Uncontrolled period-4 branch (p_4) around period 1 (p_1) in the presence of noise ($\sigma=0.005$). (c) Controlled p_{16} gets destroyed and the system jumps (shown by arrows) to p_4; $\mu_0=0.142$; $\nu=0.005$; $\sigma=0.001$. (d) Controlled noisy p_4 gets destroyed and the system jumps (shown by an arrow) to period 1; $\mu_0=0.12$; $\nu=0.005$; $\sigma=0.005$.

[6]The creation and evolution of basins in the case of the Hénon map are similar to those in the case of the Toda oscillator [16]. In this paper, we concentrate on controlling multistability, and leave the basin evolutions for a different paper.

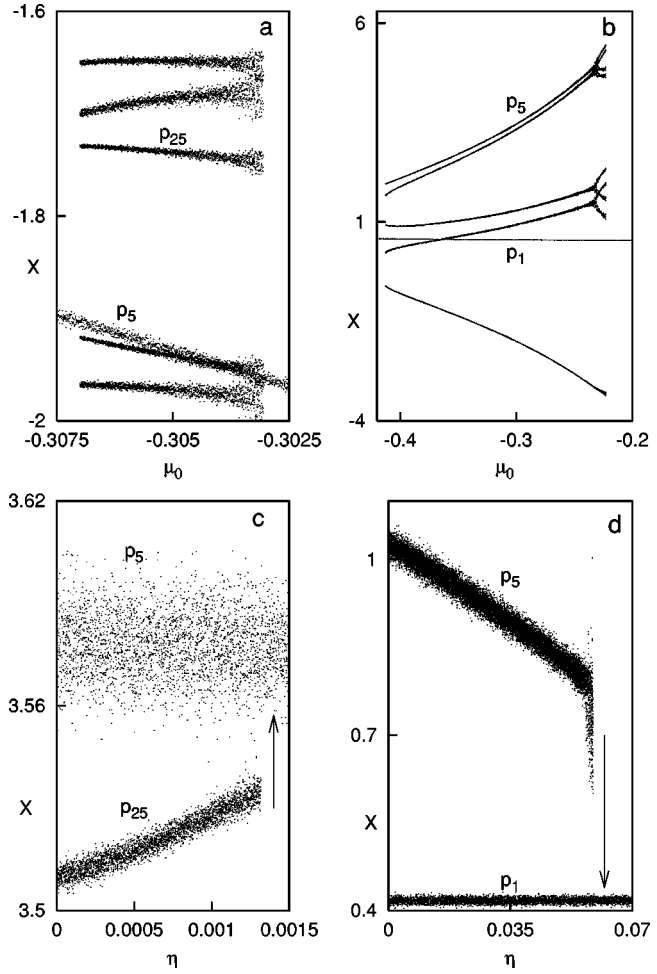

FIG. 8. (a) Uncontrolled period-25 branch (p_{25}) around period 5 (p_5) in the presence of noise ($\sigma=0.001$). Sampling period is five. (b) Uncontrolled period 5 branch (p_5) around period 1 (p_1) in the presence of noise ($\sigma=0.005$). (c) Controlled p_{25} gets destroyed and the system jumps (shown by an arrow) to the period 5; $\mu_0=0.142$; $\nu=0.005$; $\sigma=0.001$. (d) Controlled p_5 gets destroyed and the system jumps (shown by an arrow) to period 1; $\mu_0=0.12$; $\nu=0.005$; $\sigma=0.005$.

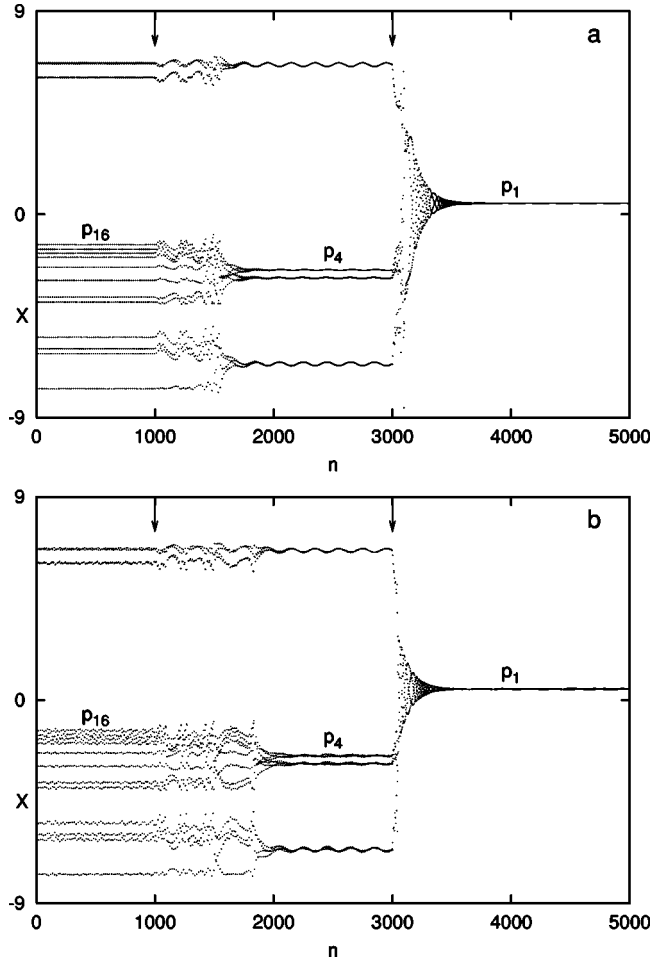

FIG. 9. (a) Sequence of controlled destructions, starting from noise-free p_{16}. Control ($\eta=0.0025,\nu=0.005,\mu_0=0.142$) is switched on p_{16} after 1000 iterations (shown by the left arrow). After destruction of p_{16}, the transients converge to p_4. Control amplitude is increased to 0.079 after next 2000 steps of iterations (shown by the right arrow). p_4 is destroyed and the iterations converge to period 1. (b) Same as (a) in the presence of noise ($\sigma=0.001$).

the effect of control on noisy p_{16} by introducing the modulation over μ. By increasing the control amplitude (η), we observe a destruction of p_{16} [Fig. 7(c)] and consequent transition to period 4 (shown by an arrow). A similar destruction can also be observed in the case of noisy p_{12} and p_{20}. Each destruction would be followed by a transition to noisy period 4 (p_4). Next, p_4 can also be destroyed by increasing the control amplitude (η) when the value of μ_0 is kept fixed anywhere, including in the parameter subintervals where the second-order secondary cascades, viz., p_{12}, p_{16}, and p_{20} exist. In Fig. 7(d), we show a typical destruction of noisy p_4 in the presence of a relatively strong noise ($\sigma=0.005$). After destruction, the transients jump (shown by an arrow) to period 1 (p_1). Figure 8 shows another similar example starting from noisy period 25 (p_{25}). Figure 8(a) shows the bifurcation diagram of the uncontrolled p_{25} branch (around period 5) in the presence of noise ($\sigma=0.001$). As we increase the value of μ_0 beyond the boundary crisis threshold of p_{25}, the transients converge to p_5. Since, the basin of period 5 is comparatively larger, the p_5 branch can withstand a relatively stronger noise. Figure 8(b) shows the bifurcation diagram of p_5 branch around period 1 in the presence of a stronger noise ($\sigma=0.005$). Beyond the boundary crisis of p_5, the transients settle to period 1 [Fig. 8(b)]. We demonstrate the effect of the control on noisy p_{25} by introducing the modulation over μ. By increasing the control amplitude (η), we observe a destruction of p_{25} [Fig. 8(c)] and consequent transition to period 5 (shown by an arrow). A similar destruction can also be observed in the case of noisy p_{20} and p_{15}. Each destruction would be followed by a transition to p_5. Next, noisy p_5 can also be destroyed by increasing the control amplitude η when the value of μ_0 is kept fixed any-

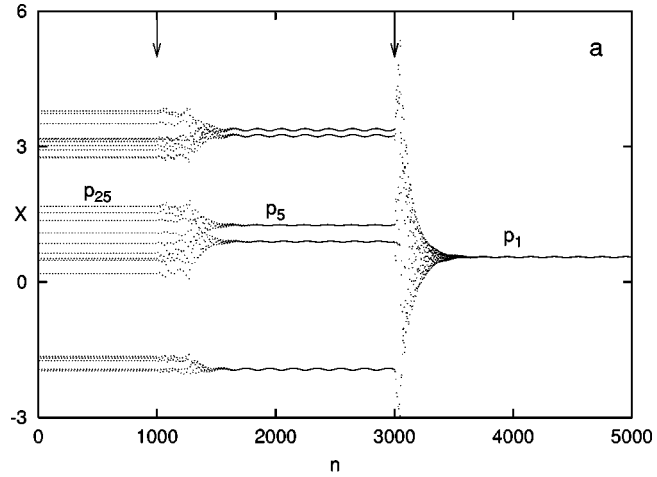

FIG. 10. (a) Sequence of controlled destructions, starting from noise-free p_{25}. Control ($\eta=0.0015, \nu=0.005, \mu_0=-0.305$) is switched on p_{25} after 1000 iterations (shown by the left arrow). After destruction of p_{25}, the transients converge to p_5. Control amplitude is increased to 0.062 after next 2000 steps of iterations (shown by the right arrow). p_5 is destroyed and the iterations converge to period-1. (b) Same as (a) in the presence of noise ($\sigma=0.001$).

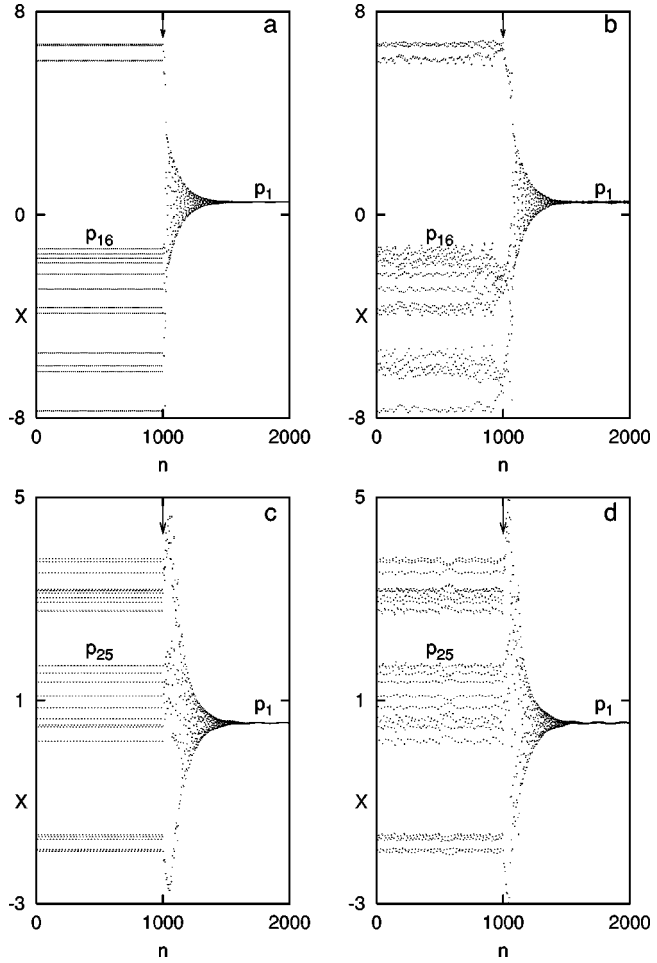

FIG. 11. Straight transition to period-1 branch after controlled destruction of the second-order cascades. (a) Control ($\eta=0.04, \nu=0.005, \mu_0=0.142$) is applied on noise-free p_{16} after 1000 steps (shown by the arrow). p_{16} is destroyed and the transients converge to p_1. (b) Same as (a) in the presence of noise ($\sigma=0.001$). (c) Control ($\eta=0.05, \nu=0.005, \mu_0=-0.305$) is applied on noise-free p_{25} after 1000 steps (shown by the arrow). p_{25} is destroyed and the transients converge to p_1. (d) Same as (c) in the presence of noise ($\sigma=0.001$).

where, including in the parameter subintervals where thesecond-order secondary cascades, viz., p_{25}, p_{20}, and p_{15} exist. In Fig. 8(d), we show a typical destruction of noisy p_5 even in the presence of a stronger noise ($\sigma=0.005$). After the destruction of p_5, the transient jumps (shown by an arrow) to period 1.

In Figs. 9 and 10 we show some typical examples of how the controlled transition from a period-n ($n>1$) branch to period-1 branch takes place in time via sequence of secondary cascades. We will show such cases with, as well as without, noise. First we consider the case of noise-free p_{16} [Fig. 9(a)]. The control amplitude is chosen higher than the destruction threshold of p_{16} and lower than the destruction threshold of p_4. The control is applied on p_{16} at 1000th iteration (shown by the left arrow). p_{16} is destroyed and the transients converge to p_4. Next, after 2000 iterations, the control amplitude is increased (shown by the right arrow) to a value higher than the destruction threshold of period 4 (p_4). Consequently, period 4 is also destroyed and the transients converge to period 1. In Fig. 9(b), we show a similar transition from a noisy period 16. The control amplitude and control frequency are identical to those in Fig. 9(a). We find that in the presence of noise also, the scenario is similar to the previous case. Figure 10 shows another example starting from a noise-free p_{25}. The chosen control amplitude is higher than the destruction threshold of p_{25} and lower than the destruction threshold of p_5. The control is switched on p_{25} at 1000th iteration [Fig. 10(a)]. p_{25} is destroyed and the transients converge to p_5. Next, after 2000 iterations, the control amplitude is increased (shown by the right arrow) to a value higher than the destruction threshold of period 5. Consequently, period 5 is also destroyed and the transients converge to period 1. In Fig. 10(b), we show a similar transition from a noisy period 25. The control amplitude and

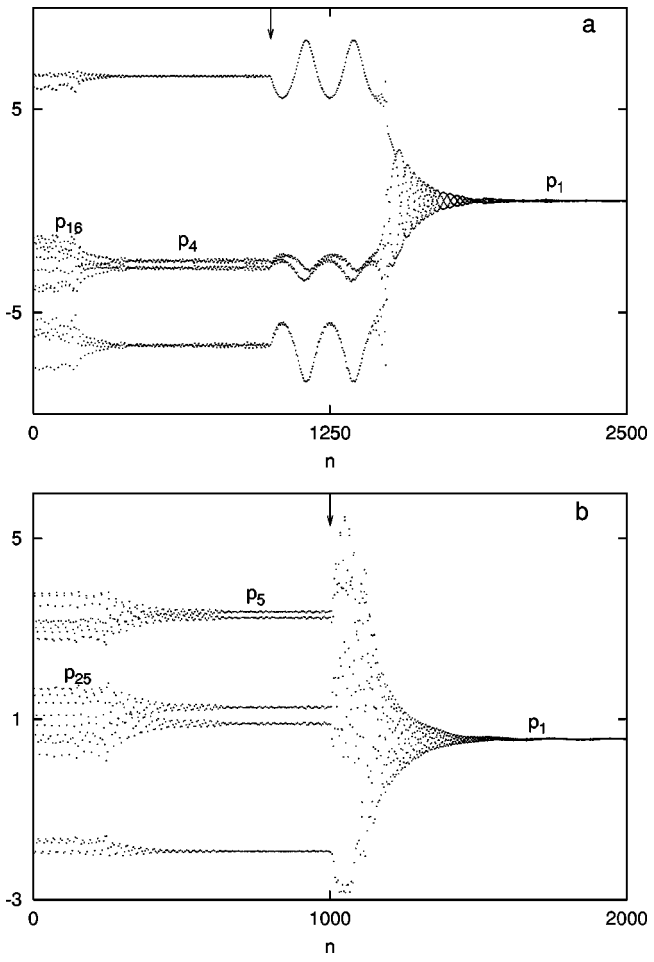

FIG. 12. Applicability of the control in the presence of relatively strong noise which spontaneously induces transition. (a) Noise ($\sigma = 0.01$) leads to a transition from period 16 to period 4. Control ($\eta = 0.04, \nu = 0.005, \mu_0 = 0.142$) is applied (shown by the arrow) on p_4 after 1000 steps of iterations. p_4 is destroyed and the transients converge to period 1. (b) Noise ($\sigma = 0.01$) leads to a transition from period 25 to period 5. Control ($\eta = 0.05, \nu = 0.005, \mu_0 = -0.305$) is applied (shown by the arrow) on p_5 after 1000 steps of iterations. p_5 is destroyed and the transients converge to period 1.

control frequency are kept identical to those in Fig. 10(a). We find that in the presence of noise also, the scenario is similar.

Next we show some typical examples of a direct transition to period 1 after a controlled destruction of the secondary cascades. Such phenomena occur when the control amplitude is set higher than the destruction threshold of the respective first-order cascade. Figure 11(a) shows the case when the control ($\eta = 0.04$) is applied on a noise-free p_{16} after 1000 steps of iterations (shown by the arrow). Since the value of the control amplitude is beyond the destruction threshold of the respective first-order secondary cascade (p_4), not only period 16 is destroyed, but also the transients straightway converge to period 1. Similar phenomena occur in the presence of noise ($\sigma = 0.001$) as well [Fig. 11(b)]. Figure 11(c) shows the controlled destruction of a noise-free period 25 (p_{25}). The control amplitude is set much higher than the destruction threshold of p_5. Therefore, after the destruction of p_{25}, the transients settle down to period 1. Similar phenomena also occur in the presence of noise ($\sigma = 0.001$) [Fig. 11(d)].

In Fig. 12 we show the applicability of the control in the presence of a relatively strong noise that can induce a spontaneous transition from one state to another. In Fig. 12(a) we consider the case starting from period 16 (p_{16}) when noise ($\sigma = 0.01$) induces a transition to period 4 (p_4). The basin of period 4 is broad enough to deter further transition to any other basin. In such a case, control needs to be applied only to destroy the lower-order cascades. Control ($\eta = 0.04$, $\nu = 0.005$) is applied (shown by the arrow) on p_4 at 1000th step of iterations. p_4 is destroyed and the transients settle to period 1. In Fig. 12(b), we show a similar example starting from period 25 (p_{25}). Noise ($\sigma = 0.01$) induces a transition to period 5 (p_5). Control ($\eta = 0.05$) is applied (shown by an arrow) on p_5 after 1000 steps of iterations. p_5 is destroyed and the transients converge to period 1. Thus, if the noise is capable of inducing a transition from the basins of higher-order secondary cascades to the basins of lower-order secondary cascades, then the control modulation is required to destroy these lower-order secondary cascades, and bring the system to period-1 branch.

To conclude, we have demonstrated that by a slow and weak periodic modulation to some system parameter, one can destroy any higher-order cascade and induce a transition to a coexisting lower-order cascade. This method can be effectively applied to bring the system from any period-n branch to period-1 branch, thus leading to a controlled monostability. Therefore, if required, such a control may also extend the operating regime. As such this method does not need any *a priori* knowledge about the destruction threshold of the various secondary cascades. Although, such knowledge could be helpful to direct a straight transition to p_1 branch. We have also shown the applicability of the method in the presence of noise. Noise of adequate strength can also induce a transition from higher-order secondary cascades to lower-order secondary cascades. Under such circumstances, control needs to be applied to bring the system from the lower-order cascades to period-1 branch.

We may also state that by an appropriate choice of the control parameter values, one can make devices with a well-defined number of coexisting states. For instance, if the control amplitude lies in between the destruction threshold of first-order and second-order cascades, one can get a controlled bistable system. We believe such an approach would be helpful for avoiding multistability when the system is designed for a bistable device. In principle, if the effect of noise is weak, by a suitable choice of control parameter values, one may even design a controlled "n-stable" device, i.e., a system that supports coexistence of $n (n = 1,2,3, \ldots)$ stable states.

We are grateful to Dr. N. Venkatramani, L&PT division, BARC, and Professor S. H. Patil, Department of Physics, IIT Bombay, for their encouragement of our work.

[1] F.T. Arecchi, R. Meucci, G. Puccioni, and J.R. Tredicce, Phys. Rev. Lett. **49**, 1217 (1982).
[2] D. Dangoisse, P. Glorieux, and D. Hennequin, Phys. Rev. A **36**, 4775 (1987); J.R. Tredicce, F.T. Arecchi, G.P. Puccioni, A. Poggi, and W. Gadomsky, *ibid.* **34**, 2073 (1987); R. Meucci, A. Poggi, F.T. Arecchi, and J.R. Tredicce, Opt. Commun. **65**, 151 (1988).
[3] H.G. Solari, E. Eschenazi, R. Gilmore, and J.R. Tredicce, Opt. Commun. **64**, 49 (1987); H.G. Solari and R. Gilmore, Phys. Rev. A **37**, 3096 (1988).
[4] V.N. Chizhevsky, J. Opt. B: Quantum Semiclassical Opt. **2**, 711 (2000).
[5] W. Lauterborn and R. Steinhoff, J. Opt. Soc. Am. B **5**, 1097 (1988).
[6] Angela Hohl *et al.*, Phys. Rev. Lett. **74**, 2220 (1996); A. Gavrielides *et al.*, Quantum Semiclassic. Opt. **9**, 785 (1997); S.K. Hwang, and J.M. Liu, Opt. Commun. **183**, 167 (1999).
[7] S. Wieczorek *et al.*, Opt. Commun. **183**, 215 (2000).
[8] F.T. Arecchi and F. Lisi, Phys. Rev. Lett. **49**, 94 (1982); **50**, 1382 (1983).
[9] M. Di Bernardo *et al.*, Int. J. Bifurcation Chaos Appl. Sci. Eng. **7**, 2755 (1997).
[10] A. Arneodo *et al.*, Physica D **6**, 385 (1983).
[11] W.L. Chen *et al.*, Int. J. Multiphase Flow **27**, 171 (2001).
[12] R.P. Kline and B.M. Baker, Int. J. Bifurcation Chaos Appl. Sci. Eng. **5**, 75 (1995).
[13] B. Barnes and R. Grimshaw, Int. J. Bifurcation Chaos Appl. Sci. Eng. **7**, 2653 (1997); H. Hayashi *et al.*, Phys. Lett. A **88**, 435 (1982).
[14] John Guckenheimer and Philip Holmes, *Nonlinear Oscillations, Dynamical Systems, and Bifurcation of Vector Fields* (Springer-Verlag, New York, 1983); F.C. Moon, *Chaotic Vibrations: An Introduction for Applied Scientists and Engineers* (Wiley, New York, 1987).
[15] B.K. Goswami, Int. J. Bifurcation Chaos Appl. Sci. Eng. **5**, 303 (1995); **7**, 2691 (1997); Phys. Lett. A **245**, 97 (1998).
[16] B.K. Goswami, Phys. Rev. E **62**, 2068 (2000).
[17] Ivan Andonovic and Deepak Uttamchandani, *Modern Optical Systems* (Artec House, Norwood, MA, 1989).
[18] G.P. Agarwal, *Nonlinear Fiber Optics* (Academic, New York, 1995).
[19] Chang-Hee Lee, Tae-Hoon Yoon, and Sang-Yung Shin, Appl. Phys. Lett. **46**, 95 (1985); Y.C. Chen, H.G. Winful, and J.M. Liu, J. Opt. Soc. Am. B **47**, 208 (1985); Wan Fung Ngal and Hai-Feng Liu, Appl. Phys. Lett. **62**, 2611 (1993).
[20] T.H.J.J. Van der Hagen *et al.*, Ann. Nucl. Energy **24**, 659 (1997).
[21] M.R. Guevara, L. Glass, and A. Shrier, Science **214**, 1350 (1981); L. Glass, M.R. Guevara, and A. Shrier, Physica D **7**, 89 (1983).
[22] E. Ott, C. Grebogi, and J.A. Yorke, Phys. Rev. Lett. **64**, 1196 (1990); W.L. Ditto, S.N. Rauso, and M.L. Spano, *ibid.* **65**, 3211 (1990); R. Roy, T.W. Murphy, Jr., T.D. Maier, Z. Gills, and E.R. Hunt, Phys. Rev. Lett. **68**, 1259 (1992).
[23] T. Carroll, I. Triandaf, I.B. Schwartz, and L. Pecora, Phys. Rev. A **46**, 6189 (1992); Z. Gills, C. Iwata, R. Roy, I.B. Schwartz, and I. Triandaf, Phys. Rev. Lett. **69**, 3169 (1992); I. Triandaf and I.B. Schwartz, Phys. Rev. E **48**, 718 (1993).
[24] D.J. Christini and J.J. Collins, Phys. Rev. E **53**, R49 (1996).
[25] C. Grebogi, E. Ott, and J.A. Yorke, Physica D **24**, 243 (1987).
[26] L. Poon and C. Grebogi, Phys. Rev. Lett. **75**, 4023 (1995).
[27] A.N. Pisarchik and B.K. Goswami, Phys. Rev. Lett. **84**, 1423 (2000).
[28] M. Hénon, Commun. Math. Phys. **50**, 69 (1976).
[29] V.N. Chizhevsky and S.I. Turovets, Opt. Commun. **102**, 175 (1993); V.N. Chizhevsky, R. Corbalán, and A.N. Pisarchik, Phys. Rev. E **56**, 1580 (1997); A.N. Pisarchik and R. Corbalán, *ibid.* **59**, 1669 (1999).
[30] C. Grebogi, E. Ott, and J.A. Yorke, Physica D **7**, 181 (1983).
[31] G.L. Oppo and A. Politi, Z. Phys. B: Condens. Matter **59**, 111 (1985); B.K. Goswami, Phys. Lett. A **190**, 279 (1994); Opt. Commun. **122**, 189 (1996).
[32] B.K. Goswami and D.J. Biswas, Phys. Rev. A **36**, 975 (1987).
[33] E. Arimondo, F. Casagrande, L.A. Lugiato, and P. Glorieux, Appl. Phys. B: Photophys. Laser Chem. **B30**, 57 (1983); A. Varone, A. Politi, and M. Ciofini, Phys. Rev. A **52**, 3176 (1995).
[34] G.L. Oppo, J.R. Tredicce, and L.M. Narducci, Opt. Commun. **69**, 393 (1989).
[35] B.K. Goswami and S. Basu, Phys. Rev. E **65**, 036210 (2002).
[36] E. Eschenazi, H.G. Solari, and R. Gilmore, Phys. Rev. E **39**, 2609 (1989).
[37] C. Scheffczyk, U. Parlitz, T. Kurz, W. Knop, and W. Lauterborn, Phys. Rev. A **43**, 6495 (1991); R. Gilmore and J.W.L. McCallum, Phys. Rev. E **51**, 935 (1995).
[38] P. Holmes and D. Whitley, Proc. R. Soc. London, Ser. A **311**, 43 (1984).
[39] G.B. Mindlin, R. López-Ruiz, H.G. Solari, and R. Gilmore, Phys. Rev. E **48**, 4297 (1993).
[40] N.K. Gavrilov and L.P. Silnikov, Math. USSR Sbornik **17**, 467 (1972); **19**, 139 (1973).
[41] S.E. Newhouse, Topology **12**, 9 (1974); Pub. Maths IHES **50**, 101 (1979); *Lectures on Dynamical Systems*, Progress in Math Vol. 8 (Birkhaüser, Boston, 1980).
[42] C. Robinson, Commun. Math. Phys. **90**, 433 (1983).